Int. J. Heat Mass Transfer. Vol. 34, No. 8, pp. 1929–1933, 1991
Printed in Great Britain

0017-9310/91 $3.00+0.00

Directional characteristics of electrodiffusion anemometric triple-split probes

V. SOBOLÍK and O. WEIN
Institute of Chemical Process Fundamentals, 165 02 Prague 6, Suchdol, Czechoslovakia

(*Received* 29 *June* 1990)

Abstract—The theory of steady convective diffusion to a circular cylinder in cross flow shows that the directional characteristics of triple-split anemometric probes depend strongly on *Re* due to the changing wake structure in the range of medium *Re*. Resulting predictions of the directional characteristics agree well with the data for a real electrodiffusion three-segment anemometric probe.

INTRODUCTION

ELECTRODIFFUSION (ED) convective probes for measuring wall shear stresses [1] or bulk velocities [2] differ from their thermal analogues by the high values of diffusion Prandtl numbers, $Sc > 1000$. This allows the calculation of local mass-transfer coefficients for given flow kinematics by using Lighthill's formula [3]. In particular, available hydrodynamical data [4–7] about the cylinder in cross flow at medium *Re* can be used for theoretical prediction of the local mass-transfer coefficients [8].

Triple-split anemometric probes consist of a cylindrical body which is split into three equal transport-active segments [9, 10], see Fig. 1. The primary data about the three independent macroscopic fluxes to these segments can be converted into information about the kinematics of flow around the probe. In particular, this information is sufficient for determining the bulk velocity and flow direction, if appropriate calibration data, so-called directional characteristics, are available. We demonstrate a possible way of predicting the directional characteristics of these probes. The prediction is compared with the calibration data for a real ED triple-split probe [10].

THEORY

The surface distribution of the velocity gradient, $q = q(x)$, is identical with the vorticity profile at the wall. This is the only hydrodynamical information we need for the calculation of mass-transfer coefficients at high Peclet numbers. For a cylindrical body in steady two-dimensional cross flow, the local diffusion flux j under a constant diffusional driving force is given by the well-known Lighthill formula [3]

$$j(x) = \frac{D^{2/3}c}{\Gamma(\frac{4}{3})9^{1/3}} \frac{\sqrt{q(x)}}{\left(\int_0^x \sqrt{q}\,\mathrm{d}x\right)^{1/3}}. \tag{1}$$

In common, the point $x = 0$ corresponds to the forward edge of the body (or an active part of the surface of this body) and the coordinate x grows in the local direction of flow close to the surface, i.e. in the direction of the development of the diffusion layer. However, there can be two such starting points, at the forward and rear edges of the body, when a region of reverse flow behind the body (wake) emerges at higher Reynolds number. These two independently developing diffusion layers join at the separation point.

In particular, for the circular cylinder in cross flow with the separation point at $\theta = \theta_0$, formula (1) can be written in the following dimensionless form [8]:

$$Sh(\theta) = \frac{(\frac{4}{9}Sc\,Re)^{1/3}}{\Gamma(\frac{4}{3})} \frac{\sqrt{|B(\theta)|}}{\left(\int \sqrt{|B|}\,\mathrm{d}\theta\right)^{1/3}} \tag{2}$$

where

$$\int \sqrt{|B|}\,\mathrm{d}\theta = \begin{cases} \int_0^\theta \sqrt{B}\,\mathrm{d}\theta; & \text{for } 0 < \theta < \theta_0 \\ \int_\theta^\pi \sqrt{(-B)}\,\mathrm{d}\theta; & \text{for } \theta_0 < \theta < \pi \end{cases} \tag{3}$$

This equation can be integrated further to obtain the expression for the partial flux to a macroscopic part of the surface

$$G(\theta) = \begin{cases} K\left(\int_0^\theta \sqrt{|B|}\,\mathrm{d}\theta\right)^{2/3}; & \text{for } 0 < \theta \leqslant \theta_0 \\ K\left(\int_{\theta_0}^\theta \sqrt{|B|}\,\mathrm{d}\theta\right)^{2/3} + G(\theta_0); & \text{for } \theta_0 < \theta \leqslant \pi \end{cases} \tag{4}$$

where

$$K = (\tfrac{3}{2}Sc\,Re)^{1/3}/\Gamma(\tfrac{4}{3}). \tag{5}$$

There are only a few sources of analytic information

NOMENCLATURE

B	dimensionless velocity gradient, qR/U
c	concentration difference between bulk and surface
D	coefficient of diffusion
$G(\theta)$	integral Sherwood number for a macroscopic part of the surface, $\int_0^\theta Sh\,\mathrm{d}\theta$
I, I_k	normalized flux to a segment dependent on α
I_{max}, I_{min}	maximum and minimum values of $I = I(\alpha)$
j	local diffusion flux
$Sh(\theta)$	local Sherwood number, $2Rj(x)/Dc$
q	velocity gradient at surface, $d_r v_\theta\|_{r=R}$
R	radius of circular cylinder
Re	Reynolds number, $2RU/\nu$
Sc	Schmidt number, D/ν
U	velocity of bulk flow
x	longitudinal coordinate on the surface, starting at the forward edge of the diffusion layer.

Greek symbols

α	directional angle for a given segment
θ	angular coordinate in polar cylindrical system
θ_0	angular coordinate of the separation point
ν	kinematic viscosity.

about the surface velocity gradient among a vast body of papers, devoted to low Re hydrodynamics of two-dimensional flows.

The result of the asymptotical analysis for $Re \to 0$, given by Illingworth [4], can be rearranged to the following expression for $B(\theta)$:

$$B(\theta) \approx (2/S)\sin(\theta) + 0.25Re(1-1/S)\sin(2\theta)$$
$$S = \ln(8/Re) - 0.077215. \qquad (6)$$

Formulas (6) predict the wake onset approximately at $Re = 6$, in agreement with the numerical analyses [5, 7].

The data about the wall shear rates, $B = B(\theta)$, in the region of medium Reynolds numbers, $1 < Re < 100$, were found in refs. [5–7]. The following representation fits these data with an acceptable accuracy:

$$B(\theta) \approx \sum_{k=1}^{3} a_k(Re)\sin(k\theta). \qquad (7)$$

The coefficients $a_k(Re)$ were determined by a least-square method and then correlated in the following way:

$$a_1 = Re^{0.75}/(0.879 + 0.614Re^{0.5})$$
$$a_2 = Re/(4.358 + 1.089Re^{0.5} + 0.054Re)$$
$$a_3 = Re^{0.5}/(865.8 + 64.8Re). \qquad (8)$$

This empirical representation should not be extrapolated outside the proper range, $1 < Re < 100$. The longitudinal profiles of $B(\theta)$, recalculated by using equations (7) and (8), are shown in Fig. 2.

The corresponding profiles of local Sherwood numbers can be calculated directly from equations (2) and (7) by numerical quadrature. For the limiting case of the forward critical point, $\theta \to 0$, formula (2) simplifies to

$$Sh(0) = K(\tfrac{4}{9}B'(0))^{1/3} = 0.978[Re\,Sc\,B'(0)]^{1/3} \qquad (9)$$

where $B'(0) \equiv \mathrm{d}B/\mathrm{d}\theta|_{\theta=0}$. Calculating $B'(0)$ from formulas (7) and (8), fitting it by a power-law on the

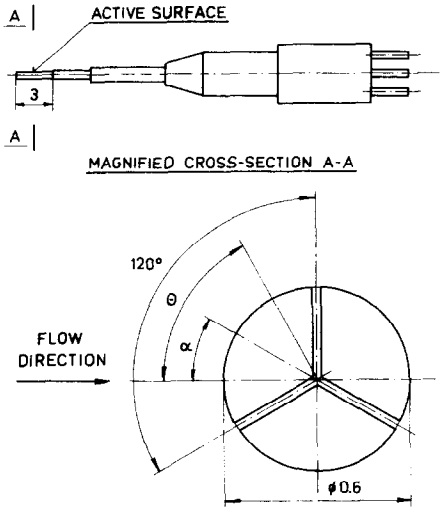

FIG. 1. Electrodiffusion triple-split anemometric probe.

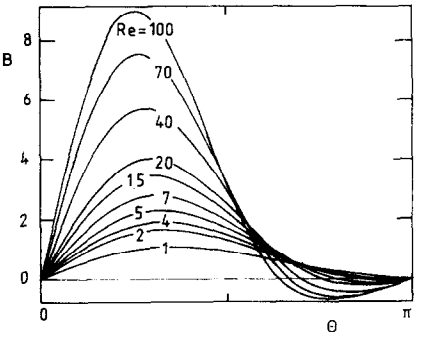

FIG. 2. Angular profiles of the dimensionless velocity gradient.

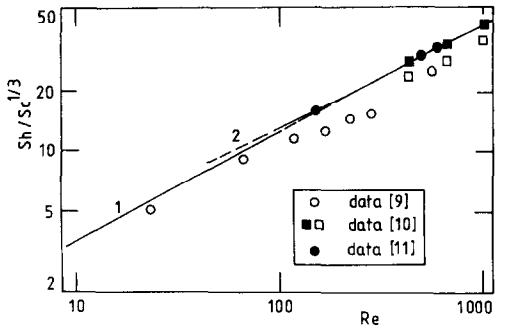

FIG. 3. Local mass-transfer coefficients at the forward edge, $Sh = Sh(0)$: (1) according to equation (10); (2) according to equation (11).

region $1 < Re < 100$, and using equation (9), one obtains

$$Sh(0)/Sc^{1/3} = 1.03Re^{0.54}. \quad (10)$$

The prediction (10) is compared with the available experimental data from refs. [11–13] in Fig. 3. The thermal data from Eckert and Soehngen [11] correspond to $Sc \approx 1$ and hence lie slightly below the theory for $Sc \to \infty$. The extrapolation of the logarithmic line (10) towards the region $200 < Re < 1000$ indicates an acceptable matching with the result of boundary-layer theory [14]

$$Sh(0)/Sc^{1/3} = 1.32Re^{0.5}. \quad (11)$$

The normalized angular profiles of $Sh = Sh(\theta)$ are shown in Fig. 4. The strong variation of their shapes, mainly due to the changing kinematics in the wake region, is of essential importance in all the considerations about the directional characteristics of the multisegment convective probes.

DIRECTIONAL CHARACTERISTICS

The directional sensitivity of multisegment convective probes is based on the aforementioned variation of local diffusion fluxes along the probe perimeter. For a single segment, this sensitivity is quantitatively characterized by the function $I = I(\alpha)$, giving an appropriately normalized current to the segment in dependence on the directional angle α. For a multisegment probe, the set of such functions for all the segments $I_k = I_k(\alpha)$ with the constraint $\Sigma I_k = 1$ constitutes the directional characteristic of the probe.

We consider an ideal cylindrical probe the surface of which is split into three identical 120° segments. Therefore, the functions $I(\alpha)$ for the individual segments differ only by the 120° shifts. The directional angle α for the single ideal segment is chosen relative to its axis of symmetry, see Fig. 1.

The theoretical prediction of directional characteristics is based on the function $G(\theta)$ giving the partial macroscopic flux to a hypothetical segment starting at the forward edge, $\theta = 0$, and ending at an angle θ. Simple symmetry considerations result in the following representation of the single directional characteristic for the ideal 120° segment:

$$\begin{aligned} 0 < \alpha < \pi/3: \quad I(\alpha) &= G^*(\pi/3+\alpha) \\ &\quad + G^*(\pi/3-\alpha) \\ \pi/3 < \alpha < 2\pi/3: \quad I(\alpha) &= G^*(\alpha+\pi/3) \\ &\quad - G^*(\alpha-\pi/3) \\ 2\pi/3 < \alpha < \pi: \quad I(\alpha) &= 1 - G^*(\alpha-\pi/3) \\ &\quad - G^*(5\pi/3-\alpha) \end{aligned} \quad (12)$$

where $G^*(\theta) \equiv \frac{1}{2}G(\theta)/G(\pi)$. An analogous approach was discussed in detail for the three-segment probes of wall friction in refs. [15, 16].

The resulting predictions of the directional characteristics of an ideal three-segment ED probe are shown in Fig. 5 for several medium values of Re. In the same figure, the experimental characteristics are shown which have been obtained by averaging the data [10] for all the three segments of a real probe. It should be noted that the experimentally obtained directional characteristics [10] exhibit an extremely high degree of symmetry which had never been attained with the thermal probes in an analogous arrangement [9].

It follows from elementary considerations that the function $I(\alpha)$ is periodic and its mean value is equal to 1/3. Let us accept that this function, smooth and

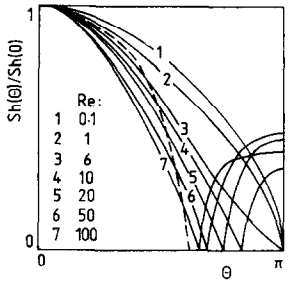

FIG. 4. Angular profiles of the normalized local mass-transfer coefficient: dashed line, boundary-layer theory [14].

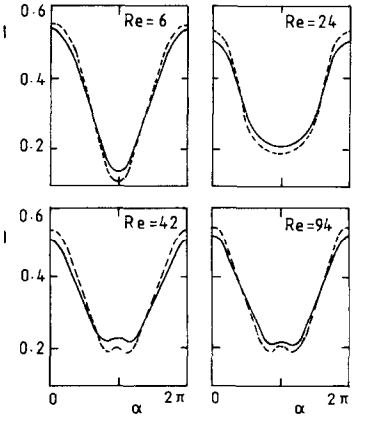

FIG. 5. Directional characteristics: dashed lines, present theory; solid lines, experiment [10].

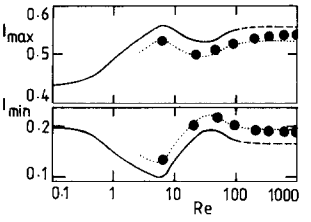

FIG. 6. Variations of I_{max} and I_{min}: solid lines, theory neglecting the insulation insertions; dotted lines, theory with a correction on the insertions; points, experimental data [10].

monotonous on the primary definition interval $0 < \alpha < \pi$, can be represented sufficiently closely by its maximum I_{max} and minimum I_{min}. These two parameters are plotted in Fig. 6 as functions of *Re*. Minor differences between the predicted and real courses of these parameters are caused by the presence of insulating insertions between the individual segments. For the real probe under consideration [10], the thickness of the insertions represents approximately 5% of the active perimeter. According to the recent theoretical analysis [17], the presence of such insertions suppresses the maximum and rises the minimum of the normalized partial currents approximately by 5% of I_{max}. The corrected estimates of the directional characteristics fit the experimental data very well, see the dotted lines in Fig. 6.

CONCLUSIONS

The directional characteristics of ED anemometric probes can be calculated from the Lighthill theory, if the corresponding steady or time-averaged flow patterns are known quantitatively for the flow region close to their surface. For the actual case under consideration, the ED triple-split probe was fabricated with such geometrical perfection that it was possible to base the theoretical prediction on the assumption of a geometrically ideal probe.

The directional characteristics change remarkably in dependence on *Re* within the range $1 < Re < 200$, due to the strong changes in the wake structure. In the range $200 < Re < 5000$, the directional characteristics remain nearly unchanged because this region of *Re* corresponds to the nearly-similarity regime of a laminar boundary layer with a stabilized wake structure. The minor difference between the prediction and data can be explained semiquantitatively by the presence of insulating insertions.

The flow fluctuations have no apparent effect on the time-averaged flow kinematics below $Re = 100$. This conclusion is based on the agreement between the theoretically predicted directional characteristics and the time-averaged reading of the ED signals.

Acknowledgements—We should like to express our thanks to the Alexander von Humboldt Foundation, Bonn, F.R.G., which made possible this work by a grant to one of us (V.S.).

REFERENCES

1. T. J. Hanratty and J. A. Campbell, Measurement of wall shear stress. In *Fluid Mechanics Measurements* (Edited by R. J. Goldstein), p. 559. Hemisphere, Washington, DC (1983).
2. V. E. Nakoryaov, A. P. Burdukov, O. N. Kashinsky and P. I. Geshev, *Electrodiffusion Method in Investigating of Turbulent Flows* (in Russian). Institute of Thermophysics, Novosibirsk (1986).
3. M. J. Lighthill, Contribution to the theory of heat transfer through a laminar boundary layer, *Proc. R. Soc. London* **202,** 359–377 (1950).
4. C. R. Illingworth, Flow at small Reynolds number. In *Laminar Boundary Layers* (Edited by L. Rosenhead), p. 180. Clarendon Press, Oxford (1963).
5. H. B. Keller and H. Takami, Numerical studies of steady viscous flow about cylinders. In *Numerical Solutions of Nonlinear Differential Equations* (Edited by D. Greenspan). Prentice-Hall, Englewood Cliffs, New Jersey (1966).
6. A. E. Hamielec and J. D. Raal, Numerical studies of viscous flow around circular cylinders, *Physics Fluids* **12,** 11–17 (1969).
7. S. C. R. Dennis and G.-Z. Chang, Numerical solutions for steady flow past a circular cylinder, *J. Fluid Mech.* **42,** 471–489 (1970).
8. B. P. LeClair and A. E. Hamielec, Viscous flow through particle assemblages at intermediate Reynolds numbers: heat or mass transport, *Inst. Chem. Engng Symp. Ser.* **30,** 197–206 (1968).
9. F. E. Jorgensen, Characteristics and calibration of a triple-split probe for reversing flows, *DISA Information* 15 (December 1981).
10. V. Sobolík, J. Pauli and U. Onken, Three-segment electrodiffusion probe for velocity measurements, *Exp. Fluids* (in press).
11. E. R. G. Eckert and E. Soehngen, Distribution of heat-transfer coefficients around circular cylinders in crossflow, *Trans. ASME* **74,** 343–347 (1952).
12. P. Grassman, N. Ibl and J. Trüb, Elektrochemische Messung von Stoffübergangszahlen, *Chemie-Ingr-Tech.* **33,** 529–533 (1961).
13. I. A. Nieva and U. Böhm, Local mass transfer for cross flow through tube banks, *Int. J. Heat Mass Transfer* **26,** 1283–1288 (1983).
14. H. Schlichting, *Boundary-layer Theory*. McGraw-Hill, New York (1960).
15. O. Wein and V. Sobolík, Theory of direction sensitive probes for electrodiffusion measurement of wall velocity gradients, *Coll. Czech. Chem. Commun.* **52,** 2169–2180 (1987).
16. C. Deslouis, O. Gil and V. Sobolík, Electrodiffusional probe for measurement of the wall shear rate vector, *Int. J. Heat Mass Transfer* **33,** 1363–1366 (1990).
17. O. Wein and K. Wichterle, Theory of segmented electrodiffusion probes: effect of insulating insertions, *Coll. Czech. Chem. Commun.* **54,** 3198–3211 (1989).

CARACTERISTIQUES DIRECTIONNELLES DES SONDES A TROIS SEGMENTS ANEMOMETRIQUES A ELECTRODIFFUSION

Résumé—La théorie de la diffusion convective permanente à un cylindre circulaire en attaque transversale montre que les caractéristiques directionnelles des sondes anémométriques à trois segments dépendent fortement de *Re* à cause de la structure à sillage changeant dans le domaine des *Re* moyens. Les prédictions des caractéristiques directionnelles s'accordent bien avec les données expérimentales pour une sonde réelle anémométrique à électrodiffusion avec trois segments.

RICHTUNGSCHARAKTERISTIKEN EINER ANEMOMETRISCHEN "TRIPLE-SPLIT" ELEKTRODIFFUSIONSSONDE

Zusammenfassung—Theoretische Analysen der konvektiven Diffusion zu einem querangeströmten Kreiszylinder zeigen, daß die Richtungscharakteristiken einer "triple-split" anemometrischen Sonde im Bereich der mittleren Reynolds-Zahlen stark durch die sich ändernden Wirbelstrukturen im Zylindernachlauf beeinflußt werden. Die theoretisch errechneten Richtungscharakteristiken stimmen sehr gut mit vergleichbaren auf einer reellen Sonde gemessenen Werten überein.

ХАРАКТЕРИСТИКИ НАПРАВЛЕННОСТИ ТРЕХСЕГМЕНТНЫХ ЭЛЕКТРОДИФФУЗИОННЫХ АНЕМОМЕТРИЧЕСКИХ ДАТЧИКОВ

Аннотация—Согласно теории стационарной конвективной диффузии для цилиндра круглого сечения, обтекаемого поперечным потоком, характеристики направленности трехсегментных анемометрических датчиков существенно зависят от значений *Re*, так как в диапазоне средних *Re* структура следа претерпевает изменения. Результаты расчетов характеристик направленности хорошо согласуются с экспериментальными данными для реальных электродиффузионных трехсегментных анемометрических датчиков.